

MTL TR 90-53

AD-A231 429

(2)

FAILURE ANALYSIS OF THE LAU-7/A LAUNCHER RETENTION BAND ASSEMBLY

DTIC FILE COPY

VICTOR K. CHAMPAGNE, Jr. and GARY WECHSLER
MATERIALS TESTING AND EVALUATION BRANCH

DANIEL A. NOWAK
MATERIALS PRODUCIBILITY BRANCH

November 1990

Approved for public release; distribution unlimited.

DTIC
ELECTED
FEB 05 1991
S E D



US ARMY
LABORATORY COMMAND
MATERIALS TECHNOLOGY LABORATORY

Sponsored by
Pacific Missile Test Center (NAVAIR)
Point Mugu, CA 93042

U.S. ARMY MATERIALS TECHNOLOGY LABORATORY
Watertown, MA

91 2 04 143

The findings in this report are not to be construed as an official Department of the Army position, unless so designated by other authorized documents.

Mention of any trade names or manufacturers in this report shall not be construed as advertising nor as an official endorsement or approval of such products or companies by the United States Government.

DISPOSITION INSTRUCTIONS

Destroy this report when it is no longer needed.
Do not return it to the originator.

UNCLASSIFIED

SECURITY CLASSIFICATION OF THIS PAGE (When Data Entered)

REPORT DOCUMENTATION PAGE		READ INSTRUCTIONS BEFORE COMPLETING FORM
1. REPORT NUMBER MTL TR 90-53	2. GOVT ACCESSION NO.	3. RECIPIENT'S CATALOG NUMBER
4. TITLE (and Subtitle) FAILURE ANALYSIS OF THE LAU-7/A LAUNCHER RETENTION BAND ASSEMBLY		5. TYPE OF REPORT & PERIOD COVERED Final Report
6. PERFORMING ORG. REPORT NUMBER		7. AUTHOR(s) Victor K. Champagne, Jr., Gary Wechsler, and Daniel A. Nowak
8. CONTRACT OR GRANT NUMBER(s)		9. PERFORMING ORGANIZATION NAME AND ADDRESS U.S. Army Materials Technology Laboratory Watertown, Massachusetts 02172-0001 SLCMT-MRM
10. PROGRAM ELEMENT, PROJECT, TASK AREA & WORK UNIT NUMBERS		11. CONTROLLING OFFICE NAME AND ADDRESS Pacific Missile Test Center (NAVAIR) Point Mugu, CA 93042
12. REPORT DATE November 1990		13. NUMBER OF PAGES 31
14. MONITORING AGENCY NAME & ADDRESS (if different from Controlling Office)		15. SECURITY CLASS (of this report) Unclassified
16. DISTRIBUTION STATEMENT (of this Report) Approved for public release, distribution unlimited.		15a. DECLASSIFICATION/DOWNGRADING SCHEDULE
17. DISTRIBUTION STATEMENT (of the abstract entered in Block 20, if different from Report)		
18. SUPPLEMENTARY NOTES		
19. KEY WORDS (Continue on reverse side if necessary and identify by block number) 25) Stainless steels, High strength steels, Spot welding / Scanning electron microscopy (SEM) ← Fatigue		
20. ABSTRACT (Continue on reverse side if necessary and identify by block number) (SEE REVERSE SIDE)		

Block No. 20

ABSTRACT

The U.S. Army Materials Technology Laboratory (MTL) conducted a comprehensive metallurgical examination of the launcher retention band assembly to determine the probable cause of failure. The assembly secures the aft end of a nitrogen receiver which is part of the LAU-7/A Guided Missile Launcher located on the F/A-18 Navy Jet. The retention band failed near the weld joint during service. Visual inspection of the assembly revealed areas conducive to crevice corrosion. Deep depressions produced by the spot welding procedure were found on the surface of the base. Wear and galling marks that were caused by fasteners that had bottomed out on the surface of the band were observed. Light optical microscopy of the fracture surfaces verified the existence of beach marks. It was determined by metallographic examination that the microstructure of the type 17-4 precipitation hardened (PH) stainless steel retention base was predominately tempered martensite with islands of ferrite while the type 301 stainless steel band showed signs of prior cold working. There was no evidence of excessive carbide formation near the weld. Chemical analysis confirmed that the retention base and band were fabricated from the specified stainless steels, AMS 5355 and ASTM A666, respectively. Hardness testing of the base showed that the minimum hardness requirement of HRC 40 was satisfied. Fractographic analysis revealed beach marks and fatigue striations. The fracture progressed in a transgranular fashion and multiple crack origins were located on the exterior surface of the band. The failure was attributed to fatigue which resulted from the combined effects of poor spot welding, excessive tensile stresses caused by fasteners which bottomed out onto the surface of the band, and the severe service conditions. The launchers have been relocated on the aircraft and are now installed on the wingtips. In this area the components are subjected to increased vibration and a more corrosive environment during service.

Accession For	
NTIS	GRA&I
DTIC TAB	<input checked="" type="checkbox"/>
Unannounced	<input type="checkbox"/>
Justification	
By _____	
Distribution/ _____	
Availability Codes	
Avail	and/or
Dist	Special
A-1	



INTRODUCTION

The LAU-7/A Guided Missile Launcher is depicted in Figure 1. The nitrogen receiver assembly is secured at two points. Towards the center of the launcher, the receiver screws into the mechanism assembly which is subsequently bolted to the launcher housing. The aft end of the nitrogen receiver is confined by the retention band assembly, as shown in Figure 2, which in turn is attached to the aft end of the launcher housing.

A detailed engineering drawing of the retention band assembly is included in Figure 3. Two components which are the focus of this investigation, the retention band and the retention base, are contained in Figures 4 and 5, respectively. The retention band was designated to be fabricated from a type 301 stainless steel and half hardened. The band was then passivated and fitted with a rubber lining. The lining, which was bonded to the inside surface of the band, was designed to provide a more secure fit against the nitrogen receiver and protect it from being galled in service. The retention base was cast from a type 17-4 PH stainless steel and subsequently hardened to HRC 40. The base was attached to the band by four spot welds according to the requirements established in MIL-W-6858.

The LAU-7/A series of launcher had been installed on the wingtips of F/A-18 jets since the early 1980's. In this location the components are exposed to a more corrosive environment and subjected to increased vibration. The previous retention spring configuration (see Figure 2) which was designed to clamp down the retention band against the nitrogen receiver, was inadequate to secure and prohibit it from rotating free from the control valve. In several instances, the retention springs also fractured. To remedy the problem a more durable liner was bonded to the inside surface of the retention band (see Figure 2) and the retention spring was fabricated from larger diameter wire stock.

During the last several weeks three retention bands have failed. The total number of recorded failures over the last two years had been approximately 30. The assembly under investigation had only been in service for less than one year before it failed during flight. There has been only one manufacturer of these components and there are approximately 6,000 retention band assemblies currently in the field.

VISUAL EXAMINATION

Figure 6 shows the retention band assembly in the as-received condition. The failure occurred at the spot-welded regions where the base, P/N 58A164C528 was joined to the band, P/N 58A164B532 (refer to lower left-hand corner of the macrograph). The inside liner which was bonded to the 301 stainless steel band experienced delamination in several places, including the area across the fracture zone. The significance of this finding was that the interface between the two parts caused by the debonding, could entrap moisture and/or an aggressive species which may initiate crevice corrosion. Another ideal situation for crevice damage was observed between the 17-4 PH stainless steel base and the band. Since spot welds were utilized to connect the parts together, the perimeter of the base was not adequately sealed off from the environment. This design provided an entrance for corrosives and a suitable haven for crevice corrosion to occur between the mating surfaces. Figure 7 reveals the fractured region from a different angle. It can be easily distinguished from this view that the failure occurred across the three spot-welds. The weld nuggets remained intact with the base while the band was completely severed from the welded assembly. The external surface of the band appeared to be free of any significant amounts of general corrosion or pitting, but

regions on the base and between the interface of the two components were attacked. Figure 8 contains a higher magnification of the area of concern. The crack propagated around the circumference of the three weld beads, within the heat affected zone (HAZ).

Figure 9 shows the general appearance of the remaining retention base that did not fail (located on the same assembly). Note the deep impressions left on the surface of the base as a result of the spot welding procedure. Corrosion pits can also be seen around the top of the three spot-welded areas. Another important observation made during the visual inspection of the component which may have contributed greatly to the overstressed condition experienced by the spot welds was found at the bottom of the two threaded portions of the base. Inspection of the retention band where screws had been inserted into the base revealed evidence indicating that these fasteners had bottomed out. The surface directly beneath the screws had been marred and gouged. The screws had actually been torqued to such an extent as to penetrate the surface of the retention band, as shown in Figure 10. This caused a greater tensile stress to exist at the spot welds and contributed to the failure.

Examination of additional randomly selected retention band assemblies verified that the spot welding procedure was not adequately controlled. Figures 11 through 13 represent the spot welds of three additional components. The welded regions of Figures 11 and 13 are much less pronounced than the deep impressions contained in Figure 12. These cavities can act as stress concentration areas where a fatigue crack could initiate.

LIGHT OPTICAL MICROSCOPY

The area of the retention band that contained the fracture was sectioned and removed from the assembly. Figure 14 shows the locations where the three weld beads had ruptured. These areas have been appropriately identified for future reference. Macroscopic examination under low magnification was utilized to determine the crack origin and to correlate fracture surface characteristics with the overall geometrical configuration of the component and the loading conditions. Figure 15 contains the fracture surface to the right of the weld bead no. 1 (refer to Figure 14 for exact location). The most important observation was the existence of beach marks which can be seen emanating from the bottom left-hand corner of the weld bead and resemble the ripples or waves that form, such as when a stone is dropped into a still body of water. Beach marks, often referred to as clamshell marks, may occur from oxidation of the fracture surfaces during periods of crack arrest from intermittent service and are associated with fatigue failures. They could also be the result of changes in loading or frequency.

Fatigue failures typically consist of three stages: crack initiation, crack propagation, and final fracture. Once a fatigue crack has been initiated, such as from a surface or subsurface defect in the HAZ, crack propagation occurs and can often times be characterized on the macroscopic scale by beach marks which represent an advancing crack front. Eventually, as the cross sectional area of the component is gradually reduced, the stress parameters of the material are exceeded and final fast fracture occurs. The fast fracture surface is usually rougher as the crack grows and the stress intensity increases.

Another series of beach marks were observed to the left of weld bead no. 1 initiating from the external surface. As their path was followed outward along the cross section of the band, a transitional zone emerged at which the beach marks were no longer visible. Beyond this point final fast fracture had taken place and the surface within this region had become

progressively coarser and more fibrous. Since the component was subjected to vibration and shock during all phases of flight, especially at final arrestment, the beach marks were a result of crack propagation during these loading and/or frequency changes in service and subsequent periods of nonusage at which time oxidation of the exposed fracture surface occurred.

Figure 16 represents the fracture surface adjacent to the right-hand side (refer to Figure 14) of weld bead no. 2. Again, evidence of beach marks was observed extending in a semi-elliptical manner from the upper right-hand surface of the retention band. This array of beach marks was the most pronounced found over any of the weld bead fracture surfaces examined. The crack origin was determined by tracing these marks back to a common center point, as identified in the macrograph. These beach marks extended outward until they met the beach marks that formed to the left of weld bead no. 3 and, therefore, the final fast fracture region was virtually nonexistent. It was deduced that because these beach marks were much more distinct and prevalent over most of the fracture surface of this weld bead, they were probably the first to form. In reconstructing the failure, it was later concluded that the primary fatigue crack initiated at the HAZ of weld bead no. 2. As the crack front gradually advanced across the entire thickness of the weld, the cross sectional area of the band decreased and the stress intensity increased as a result. Other fatigue cracks then formed on the external surfaces near weld beads no. 1 and no. 3. Final fast fracture occurred at weld beads no. 1 and/or no. 3 before a significant number of beach marks were formed on these fracture surfaces. This conclusion explains the differences observed between the clarity and the number of beach marks contained on weld bead no. 2 and the remaining weld beads.

Figure 17 shows the fracture surface of weld bead no. 3. The macroscopic features located within this region resemble weld bead no. 1 in that the beach marks are fainter than weld bead no. 2 and there exists a large fast fracture zone.

MICROSTRUCTURE

A cross section of the failure site located at weld bead no. 2 was taken and prepared for metallographic examination. The sample was etched utilizing a solution of 97% HCl and 3% HNO₃ with the addition of one half gram of CuCl₂. The resulting microstructure of the spot-welded assembly is revealed in Figure 18. The thin component is the 301 stainless steel band while the bottom part is the 17-4 PH stainless steel base. The failure occurred across the HAZ of the band at the corner of the depression made by the spot-welding electrode. Deeper cavities can be seen beneath the weld nugget and can act as stress raisers in the material. The HAZ is easily recognized at the areas which have etched darker and are characterized as the two vertical bands on either side of the weld bead. The weld nugget itself exhibits a typical dendritic structure representative of an as-cast material. Two voids can be observed near the center of the weld bead and may have been caused by entrapped gas or shrinkage.

Figure 19 shows the failure site at higher magnification. The slender bands that run horizontally across the 301 stainless steel have preferentially etched darker because of prior cold working which occurred during primary material processing. The center grains have been compressed from external rolling forces forming flow lines. Figure 20 contains the microstructure outside of the HAZ of the 301 stainless steel band, while Figure 21 reveals the structure within the HAZ. The flow lines are much more discernable at these magnifications. Recrystallization has taken place within the HAZ which is signified by a smaller equiaxed grain size.

The matrix was clean with no signs of unusual microstructural features or large defects. There was no evidence of excessive carbide formation within the material. The structure of the retention base shown in Figure 22 is predominantly tempered martensite with islands of ferrite, while that within the HAZ is characterized by a refined martensitic structure as contained in Figure 23. Both areas also contain minimal amounts of untempered martensite.

CHEMICAL ANALYSIS

The retention band P/N 58A164B532 is required to be fabricated from 301 stainless steel in the half-hardened condition, according to the requirements of QQ-S-766 "Steel, Stainless and Heat Resisting, Alloys, Plate; Sheet and Strip." The retention base P/N 58A164C528 was to conform to the material requirements established in AMS 5355 "Steel Castings, Investment, Corrosion Resistant" for 17-4 PH stainless steel. Atomic absorption (AA) and inductively coupled argon plasma emission spectroscopy (ICP) were used to determine the chemical composition of each alloy. The carbon and sulfur content was analyzed by the LECO combustion method. The specified compositional ranges for these materials have been included for comparative purposes. The chemical analyses of both components compared favorably with required values as shown in Table 1.

Table 1. COMPARISON OF CHEMISTRIES

Element	C	Mn	Si	P	S	Cr	Ni	(Co & Ta)	Al	Cu	Sn	N
Base	0.04	0.42	0.91	0.018	0.022	16.2	4.45	0.25 + 0.10	0.04	3.57	0.015	0.04
AMS 5355	0.06 Max	0.70 Max	0.5 Min. 1.0 Max	0.04	0.03	15.5 16.7	3.6- 4.6	0.15- 0.40	0.05	2.8- 3.5	0.02	0.05
Band	0.115	1.2	0.5	0.027	<0.001	17.0	7.25					
ASTM A666	0.15	2.0 Max	0.75 Max	0.045 Max	0.03 Max	16.0 18.0	6.0 8.0					0.10

HARDNESS TESTING

A sample of the cast 17-4 PH stainless steel retention base was sectioned from the component and mounted in bakelite. The specimen was subsequently polished and prepared for hardness testing. The engineering drawing of the part requires a minimum hardness of HRC 40. The measured values of hardness compared favorably with specified requirements and the tests did not reveal evidence of any significant variations (see Table 2).

Table 2. MACROHARDNESS MEASUREMENTS

HRC 500 Kg Load Diamond Indentor	
Number of Readings	HRC
1	37.3
2	39.6
3	39.8
4	39.9
5	39.5
6	39.7
7	39.9
8	40.3
9	40.4
10	40.6
11	40.9
12	40.5
13	40.8
14	39.9

Average = 39.9 Standard Deviation 0.88

FRACTOGRAPHY

The fracture faces of the retention band were examined at a higher magnification utilizing the scanning electron microscope (SEM) in order to identify the failure mode in each of the three weld bead areas. Figure 24 shows the fracture surface within area 1 of weld bead no. 2 (identified previously on Figure 14). Well-defined beach marks are clearly distinguishable on the fractograph. The arrow points to the possible origin of the fatigue crack which is the common point where the beach marks converge. The surface near the crack nucleation site was relatively smooth and flat faced. Closer examination of the crack initiation site did not reveal any evidence of an inclusion or a surface defect, such as a corrosion pit.

Figure 25 represents area 2 located near the same weld bead approximately 180° away from area 1. The beach marks observed in this region extend outward in an opposing direction to those contained in Figure 24. Another notable feature which was observed to the right of the crack origin (designated by the arrow) was parallel steps extending vertically across the thickness of the weld bead. These same markings were also found to the left of the crack initiation site contained in Figure 24 and are shown at higher magnification in Figure 26. These macroscopic patterns were the result of an advancing crack front which expanded across different planes.

Figure 27 verifies that the fracture mechanism near the crack origin was transgranular in nature, where crack growth proceeded along crystallographic planes. Further examination of

various regions within the beach marks and across the fast fracture zones of weld beads no. 1 and no. 3 displayed similar topographies. A transgranular mode of fracture in this type of material is often associated with fatigue failures. In polycrystalline materials, a transgranular fracture propagates through grains that are randomly oriented with respect to one another and, therefore, will continually change direction as it crosses grain boundaries. Inherent material defects, such as inclusions or precipitates, further complicated the fracture path producing unique marks on the fracture surface that are readily associated with this type of fracture mechanism.

The most prominent features associated with fatigue failures are finely spaced parallel marks referred to as striations, as shown in Figure 28. Fatigue striations are the result of a single cycle of stress and are a visual record of the position of the fatigue crack front as it propagates through the material. Figures 29 and 30 contain further examples of fatigue striations near the crack origin of weld bead no. 2, while those in Figure 28 were found in an area located before the final fast fracture zone of weld bead no. 3. The difference in appearance between the two sets of striations was significant. Those near the crack initiation site were very well defined and continuous being found on a relatively smooth surface. The striations observed far beyond the origin were located on a much more fibrous fracture surface and were less pronounced. Figure 31 shows the uniform appearance of a series of striations also located near the crack nucleation site. Fatigue striations generally increase in spacing as they proceed away from the origin aligned perpendicular to the microscopic direction of crack propagation. The black spots evenly distributed across the fracture surface were corrosion product as characterized by energy dispersive spectroscopy (EDS). The EDS spectra shown in Figure 32 contains those elements associated with the type of steel under investigation such as Si, S, C, Cr, Fe, Al, and Ni, as well as oxygen which is indicative of a corrosion product. In addition to being elemental additives of the steel, the Si, S, and C peaks may also be attributed to surface lubricants and oils. The existence of Cl, Na, K, and Mg represents those elements commonly found in salt water and were anticipated since the component was exposed to a marine environment.

When examining the surface edge of area 3, positioned between weld beads no. 2 and no. 3, multiple cracks were observed side by side originating from the surface as shown in Figure 33. Multiple crack sites are associated with corrosion fatigue but there was no evidence of corrosion pitting and the crack origin was clearly visible. Often the crack initiation site of a corrosion fatigue fracture is indistinct because the compression portion of each stress cycle has forced corroded mating surfaces together behind a irreconcilable fracture surface. Figures 34 and 35 are SEM fractographs showing secondary cracks which were observed within the HAZ of all the weld beads. Corrosion fatigue failures may display cracks or fissures perpendicular to the primary fatigue crack. These secondary fractures were confined only to the HAZ of the weld beads. Metallographic specimens sectioned from areas adjacent to and beyond the HAZ and further fractographic examination within similar regions did not reveal further signs of cracking. This evidence suggests that the stresses induced into the component during spot welding caused these fractures which may have initiated at carbides.

The failure mechanism and surface morphology of the remaining weld beads were consistent with those of weld bead no. 2 with the exception of the appearance of the beach marks and the size of the final fast fracture zone. Figure 36 shows the beach marks found in area 4 of weld bead no. 3 which were significantly fainter and less pronounced. In addition, the fast fracture zone of weld beads no. 1 and no. 3 were larger. The surface topography within the fast fracture regions were expected to display evidence of dimples which are indicative of

overload conditions during fractures. However, because the 301 stainless steel band had been significantly rolled during material processing, the resulting elongated grains made it difficult to resolve a dimpled surface.

DISCUSSION

The failure of the retention band assembly was attributed to fatigue cracks which initiated at multiple sites within the HAZ of the spot welds. The cracks originated and propagated from the external surface of the retention band exposed to the environment. Examination of the spot welds contained on this component as well as other fielded retention assemblies revealed that the resistance welding procedure was inadequately controlled and sometimes caused surface cavities. These defects provided stress concentration areas at which fatigue cracks originated due to alternating service loads. Excessive tensile stresses were also induced at the spot-welded regions as a result of fasteners which were threaded into the retention base and had bottomed out onto the surface of the band. In addition, corrosion may have increased the propagation rate of existing fractures, but the mechanism of corrosion fatigue (CF) was not concluded as being the predominant factor in this failure. The crack initiation sites of CF failures are often obscured by corrosion products and the surface morphology in these regions are often irreconcilable. This investigation did not reveal evidence of any such features.

Another failure mechanism associated with austenitic stainless steels is sensitization. This occurs when the materials is exposed to a temperature of approximately 1000°F to 1550°F causing the precipitation of chromium carbides at the grain boundaries. The material becomes susceptible to intergranular attack because areas within the grain boundaries become depleted of chromium which provides the corrosion resistance for the stainless steel. Preferential attack takes place at the grain boundaries when the component is exposed to appropriate environmental conditions (i.e., salt water, moisture, etc.) causing cracking under stress due to intergranular decohesion. However, intergranular cracking was not observed on the fracture surfaces of the component and there were no excessive carbides revealed.

CONCLUSIONS

1. Visual examination of the component revealed areas conducive to crevice corrosion, such as the inside liner and retention band interface, as well as the surface between the retention base and the band. The spot welds produced depressions on the surface of the base resulting in stress concentration regions. The fasteners threaded into the base bottomed out on the retention band causing excessive tensile stresses at the spot welds. Corrosion pits were also observed in various areas of the base.
2. Light optical microscopy of the fracture surface showed the existence of beach marks which are associated with fatigue failures. The fracture faces were relatively clean with very little signs of corrosion. The crack origins could be determined by following the progression of beach marks back to a center point.
3. The microstructure of the retention band showed prior cold working. The failure occurred at the HAZ. The weld nuggets exhibited a typical dendritic, as-cast structure. The retention base showed a predominantly tempered martensite structure with islands of ferrite consistent with specified requirements. There was no evidence of excessive carbide formation.

4. Chemical analysis confirmed that the retention base was fabricated from a 17-4 PH stainless steel according to the requirements established in AMS 5355 while the retention band conformed to the chemical composition of 301 stainless steel as specified in ASTM A666.

5. Hardness testing of the retention base showed that the minimum hardness of HRC 40 designated on the engineering drawing had been satisfied.

6. Fractographic analysis of the fracture faces confirmed that the failure was attributed to fatigue by the observance of beach marks and fatigue striations. The fracture mode was transgranular which is also indicative of fatigue. Multiple crack origin sites initiated from the external surface of the retention band within the HAZ of the spot welds.

RECOMMENDATIONS

It is not the intent of this investigation to provide specific guidance on the prevention of fatigue failures involving the retention band assembly. However, there are certain measures that can be implemented immediately which will help to alleviate some of the conditions that promoted this failure based upon the results presented in this report.

General Preventive Measures

1. The resistance welding process must be controlled to insure uniform, high quality spot welds. The important variables involved include, but are not limited to, the following:

- Careful alignment of the welding electrodes to the component insures an evenly distributed weld current.
- Constant weld current should be maintained to achieve the necessary thermal gradient within the work pieces and should promote uniform cooling and minimum carbide formation.
- The duration of the weld should be consistent for each weld (both the applied current and cooling cycles) to yield uniform weld nuggets and to allow for a balanced stress field distribution in service.
- Uniform electrode force should be applied to prevent blow hole formation.
- Weld surfaces should be properly cleaned to provide uniform resistance. The retention band and base contain passivated oxide layers which need to be removed prior to welding. This chromium oxide layer is a refractory material and has a high melting temperature. In addition, surfaces greases and oils can cause inclusions and porosity, as well as alter the chemical composition within the weld.
- The proper spacing of spot welds must be insured to prohibit shunting of current through an adjacent weld nugget preventing proper fusion of the subsequent weld attempt. To compensate, the welding current must be increased for the next spot weld.

Note that if these parameters are properly maintained the degree of variability between the components will decrease enhancing the overall reliability of the production run. Controlling some of these important variables with the required repeatability can be achieved with an automatic controller which is connected in series to the resistance weld unit. This allows one

to fine tune the weld schedule and continually yield the desired weld by precise control of the applied weld current and coolant.

2. The retention attaching screw, and the blast shield and retention assembly attaching screw, should not be allowed to bottom out onto the surface of the retention band creating excessive tensile stresses at the spot weld regions.

3. If fatigue failures continue to occur after 1 and 2 above are implemented, this may indicate that the spot welds do not have adequate strength to withstand the service conditions and may not be the proper welding process for this application. In addition, corrosion within sites previously identified may be initiating fatigue cracks. The LAU-7/A series of launchers have been installed on the F/A-18 wingtips, since the early 1980's, which is a more damaging location. The launchers are exposed directly to the environment and are subjected to an increased amount of mechanical vibration and shock loading. These factors can decrease the fatigue life of the spot welds, especially if corrosion becomes involved in the mechanism of failure, as shown in Figure 37.

To combat these problems an alternative welding process and/or a redesign of the component should be considered (i.e., alternative materials). The information required to accomplish this would consist of the following:

- Evaluation of the loading conditions of the assembly.
- Selection of proper alternative materials of the retention band and base that combine good weldability with adequate strength and corrosion resistance properties.
- Determination of the proper welding process for the application.
- Conduct procedure qualifications that will test the strength of the weld and its performance out in the field.

ACKNOWLEDGMENTS

The author wish to extend appreciation to CPT John Beau. PhD, and Dr. Shared Pednekar for their helpful discussions.

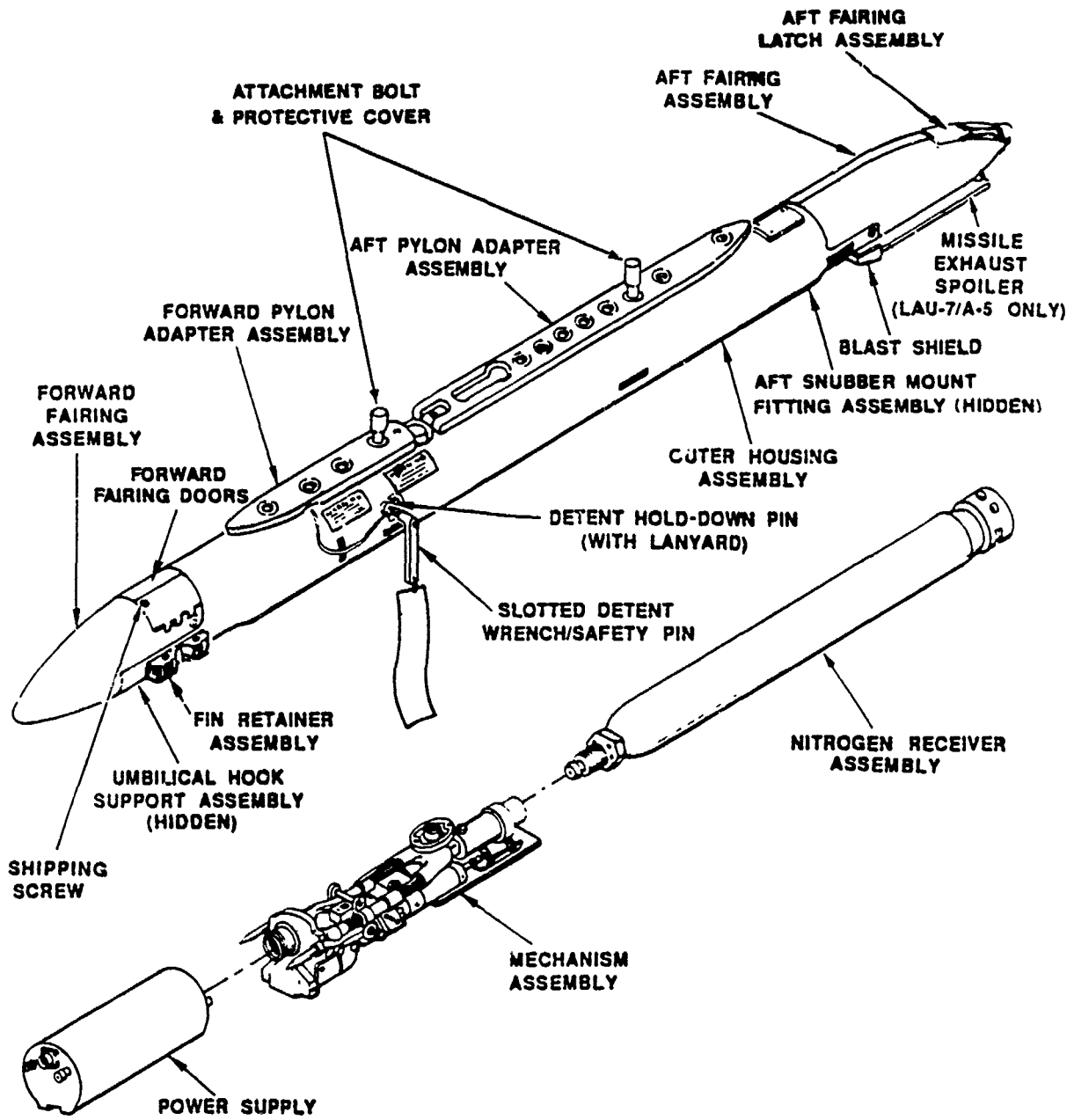


Figure 1. Illustration of the LAU-7/A Guided Missile Launcher assemblies.

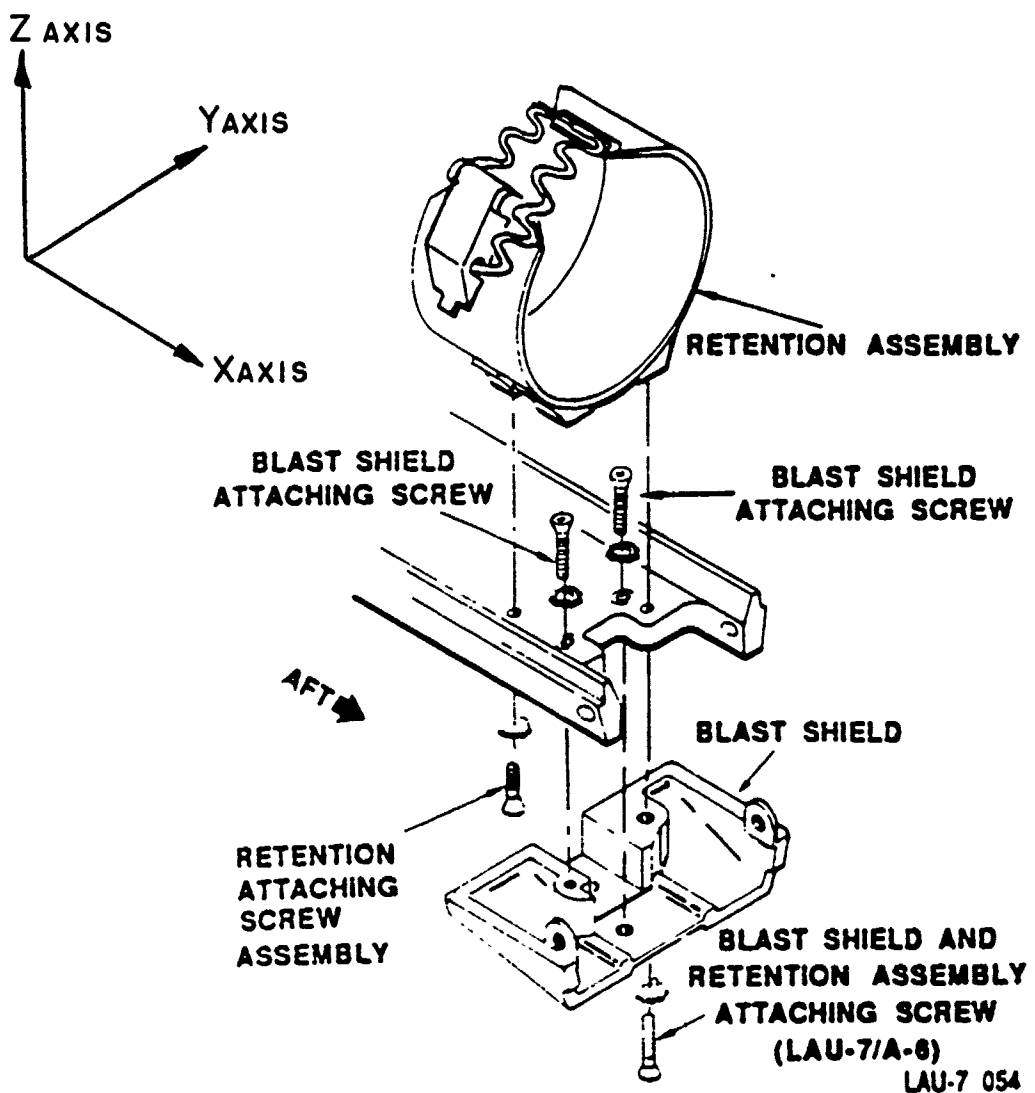


Figure 2. Schematic showing the retention band assembly.

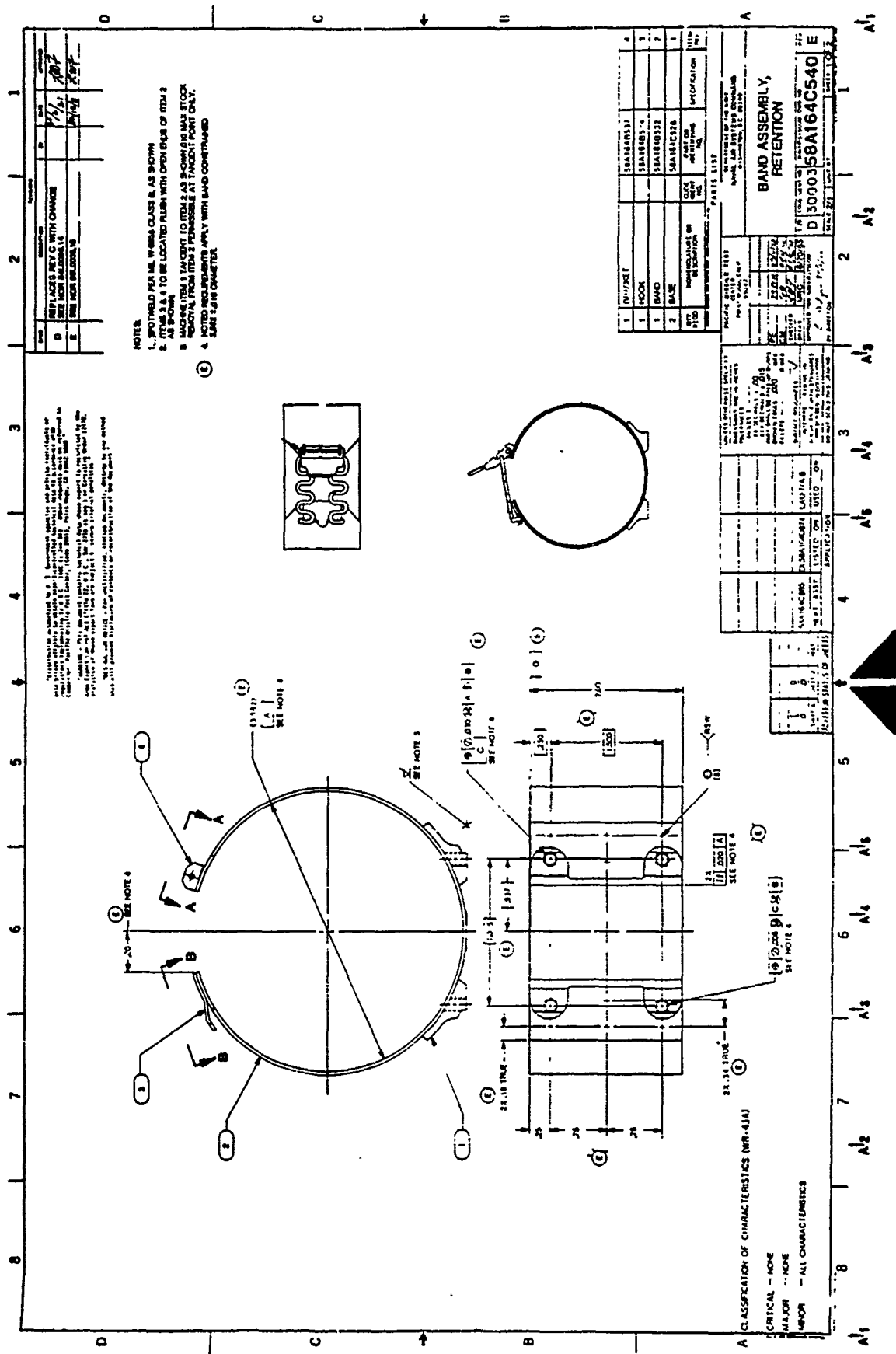


Figure 3. Engineering drawing of the retention band assembly.

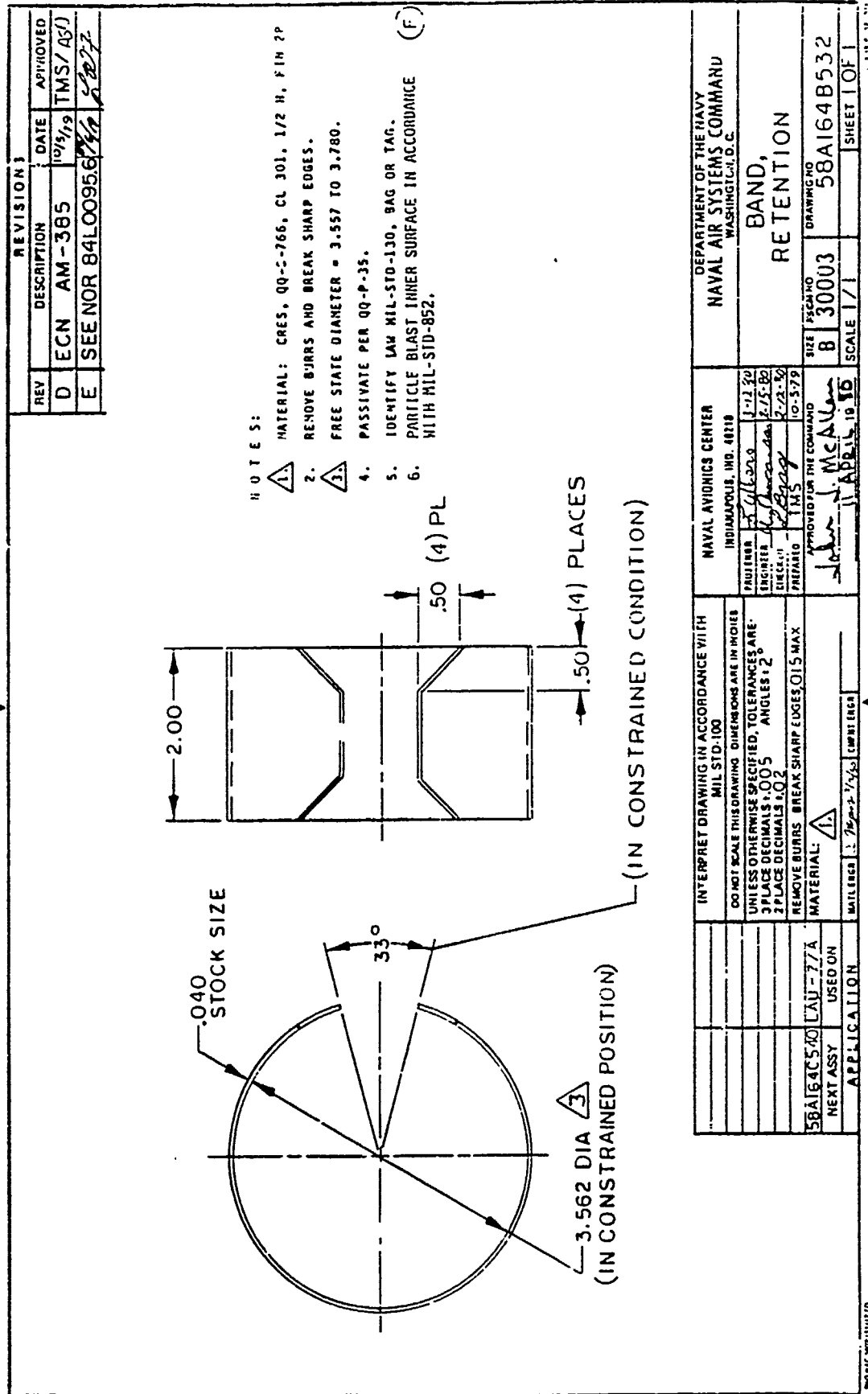


Figure 4. Engineering drawing of the retention band.

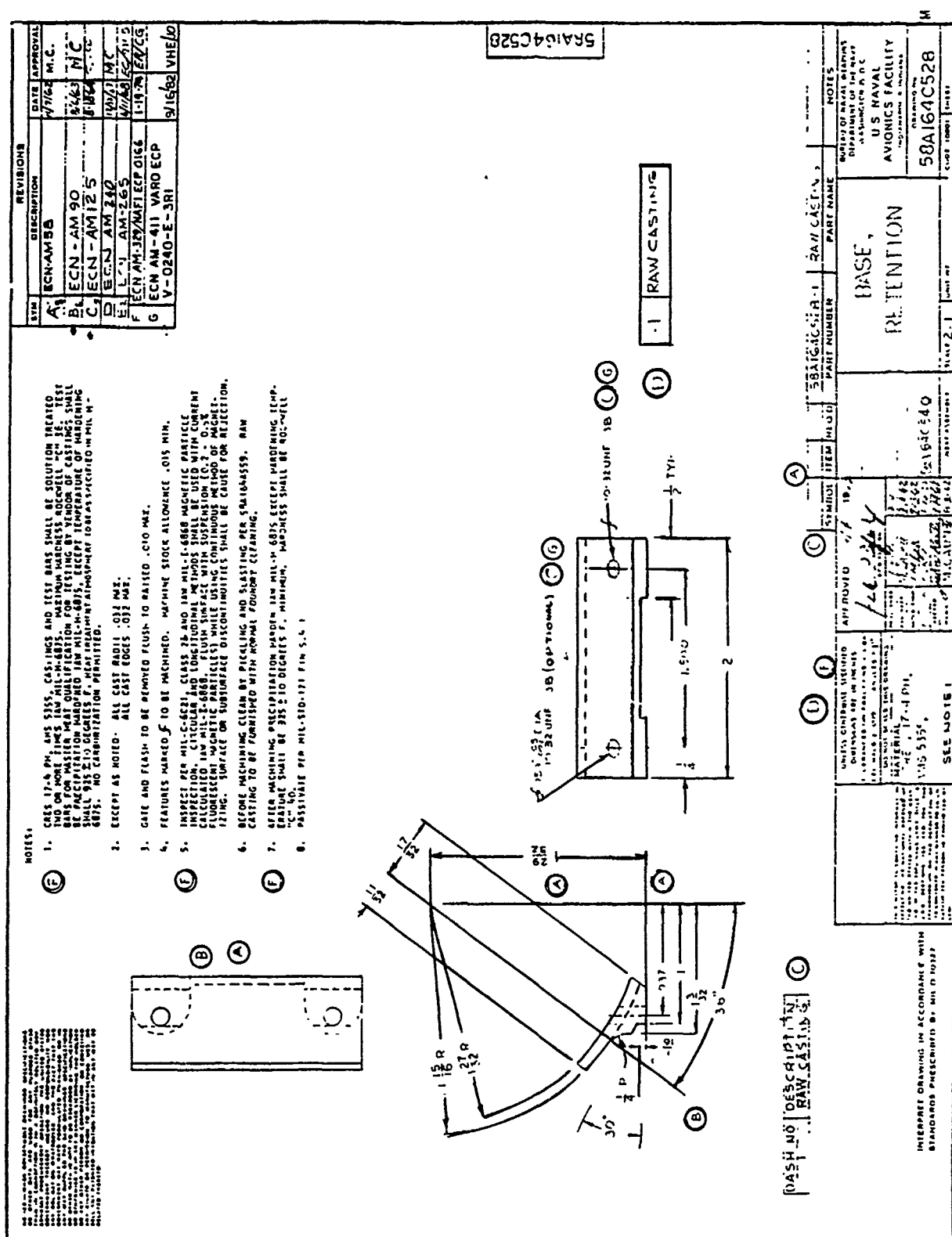


Figure 5. Engineering drawing of the retention base.

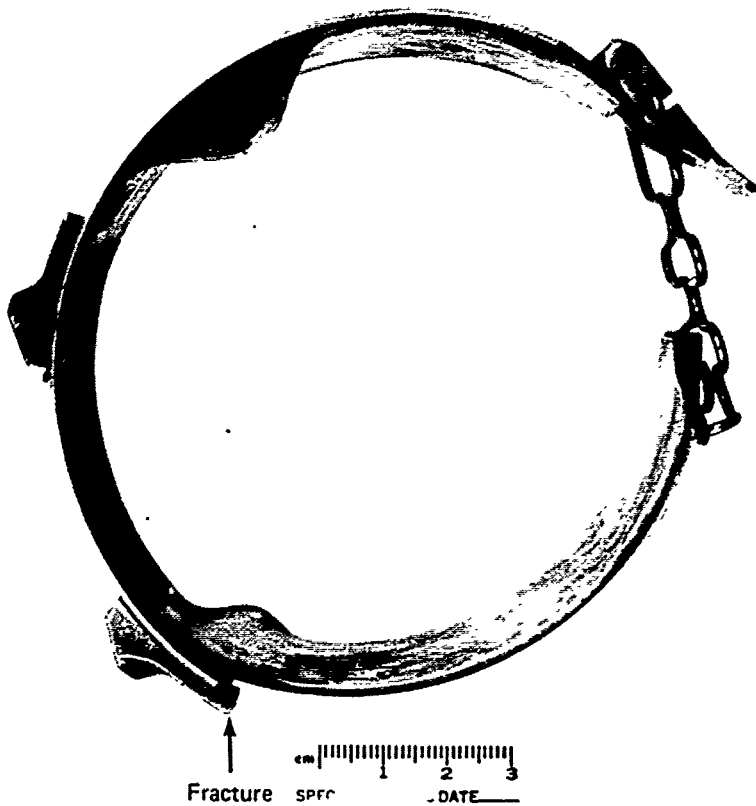


Figure 6. Shows the retention band assembly in the as-received condition.

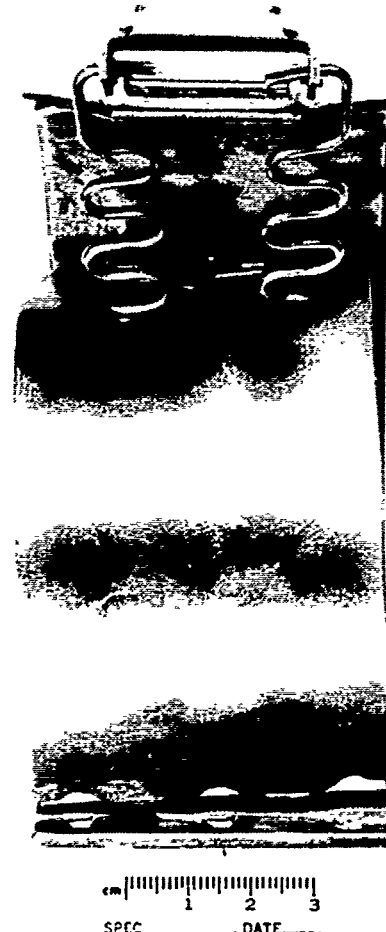


Figure 7. Reveals the fracture which occurred across three spot welds used to attach the retention base to the band.



Figure 8. Contains the failed spot welds at higher magnification. Mag. 2.2X

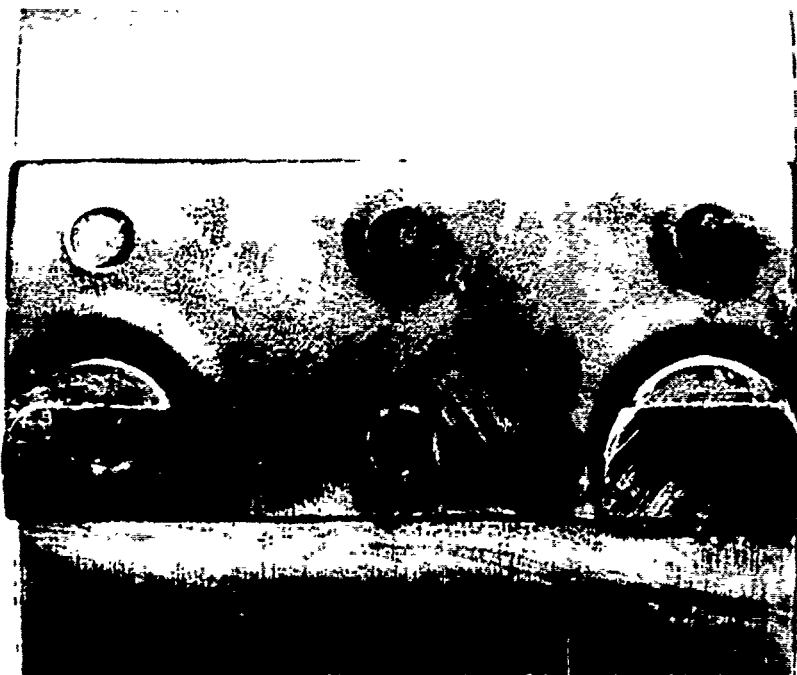


Figure 9. Shows the deep impressions left on the surface of the base as a result of the welding procedure. Mag. 2.2X



Figure 10. Macrograph of the retention band surface where an attachment screw had bottomed out, gouging the material. Mag. 10X

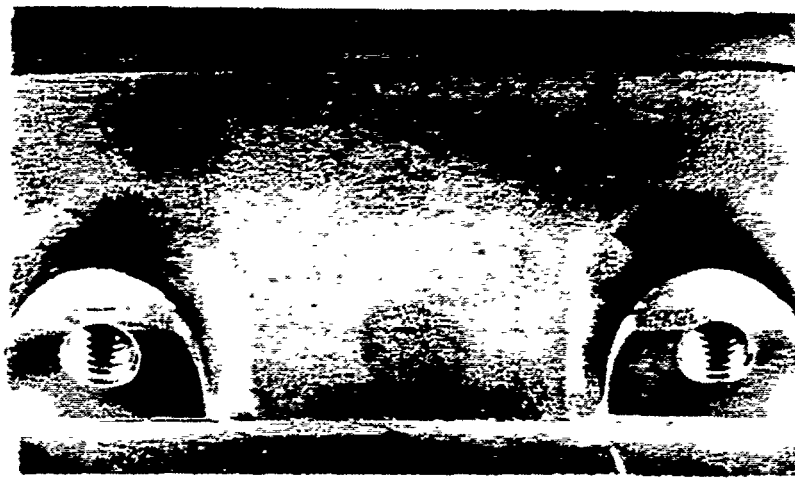


Figure 11.

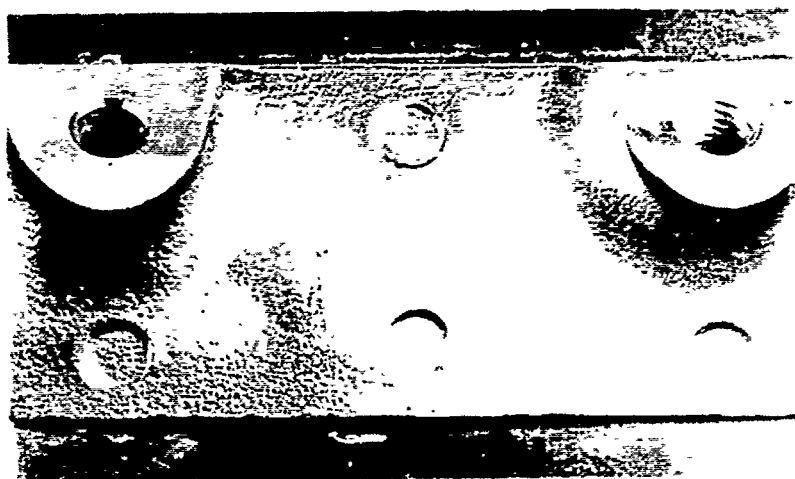


Figure 12.

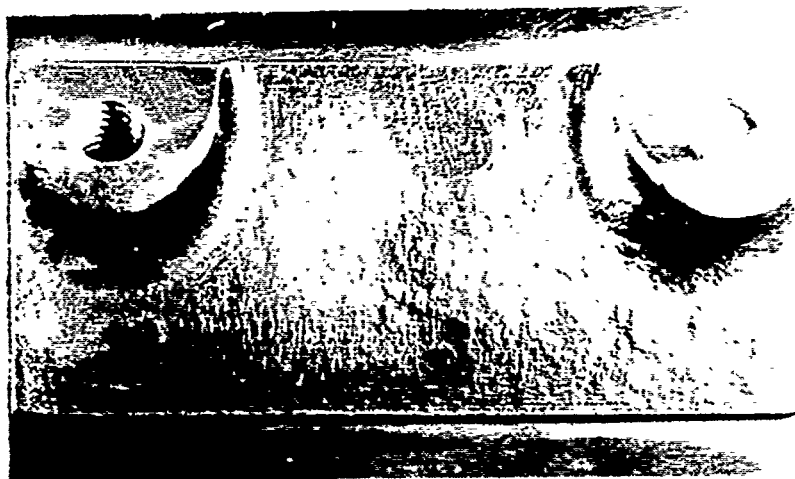


Figure 13.

Figures 11 through 13. Optical photographs showing spot welded regions of three separate retention bands. Note that the surface depressions occur randomly, indicative of a welding process that had not been adequately controlled. Mag. 2.2X

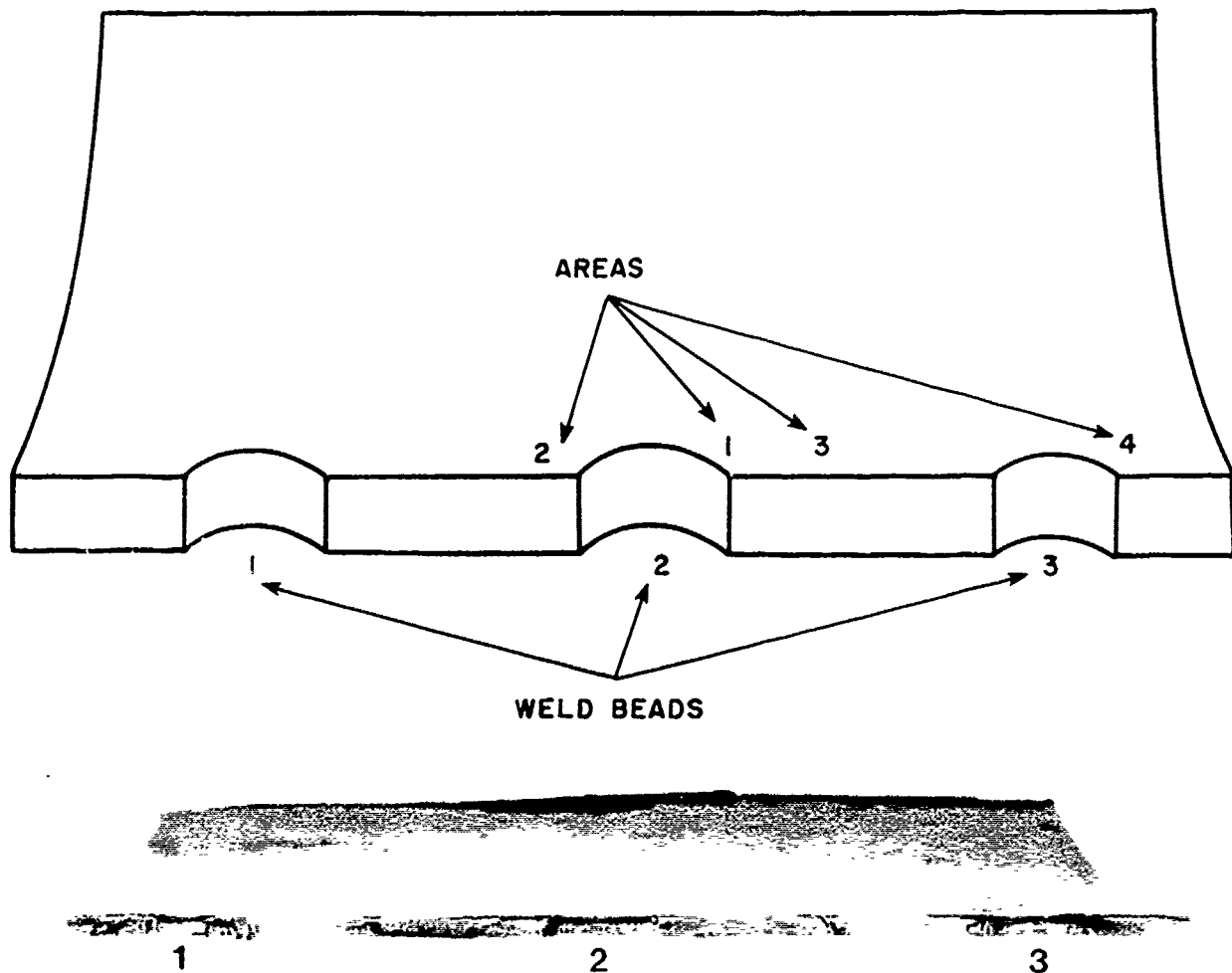


Figure 14. Shows the location of the failure where the three weld beads had ruptured. Mag. 3X



Figure 15. Shows optically the fracture surface of the area located to the right of weld bead no. 1. Mag. 11X



Figure 16. Shows optically the fracture surface of the area located to the right of weld bead no. 2. Mag. 11X



Figure 17. Shows optically the fracture surface of the area located to the right of weld bead no. 3. Mag. 11X

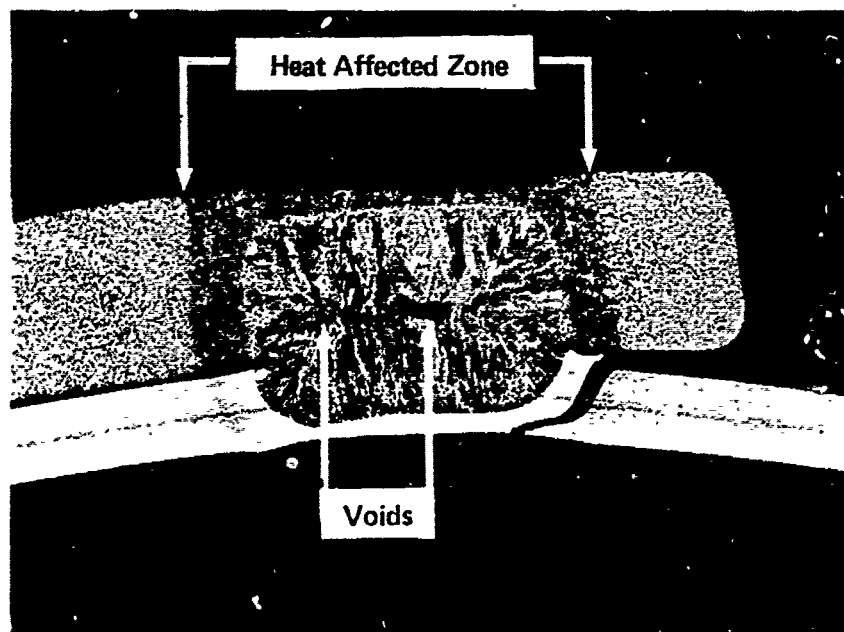


Figure 18. Reveals the microstructure of the failed spot-welded assembly.
Note the failure occurred within the HAZ. Mag. 10X

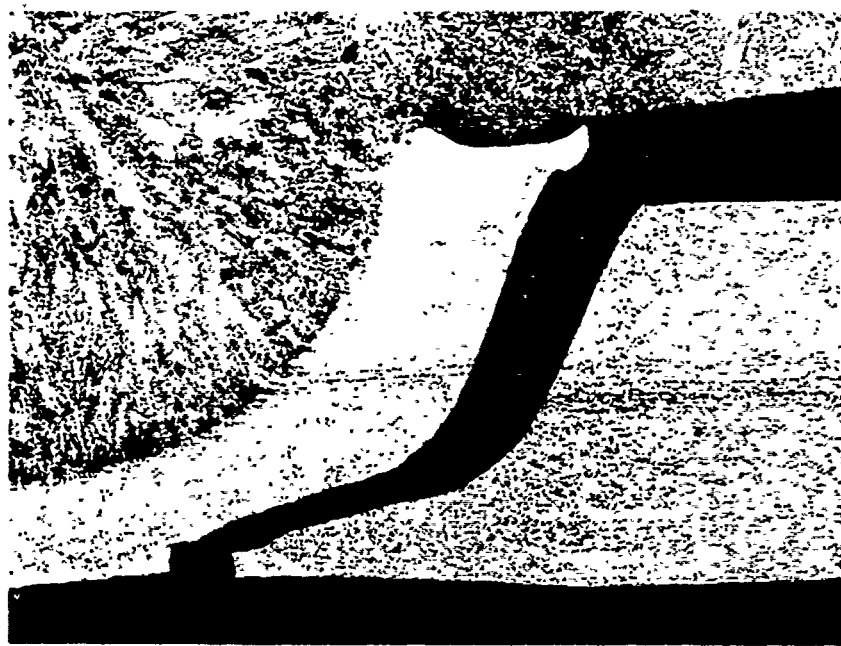


Figure 19. Higher magnification of the failure region showing flow lines at the center of the band. Mag. 50X

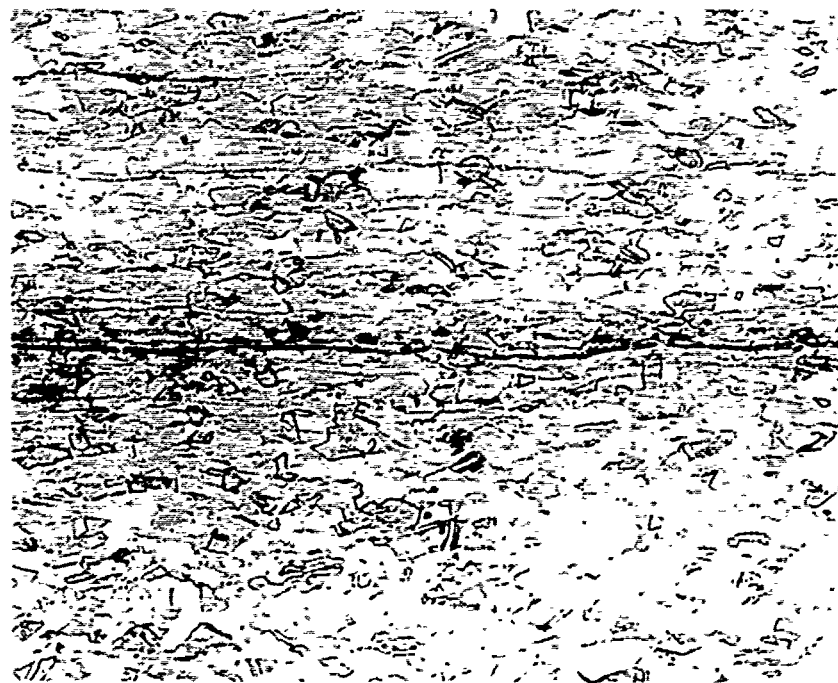


Figure 20. Microstructure of the 301 stainless steel band outside of the HAZ. Mag. 200X

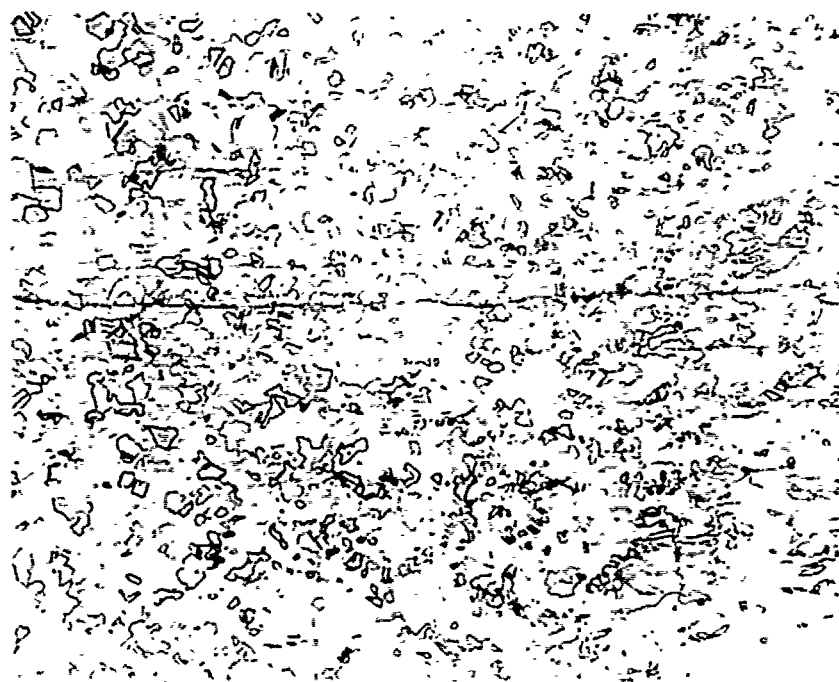


Figure 21. Microstructure of the band within the HAZ showing evidence of recrystallization. Mag. 200X

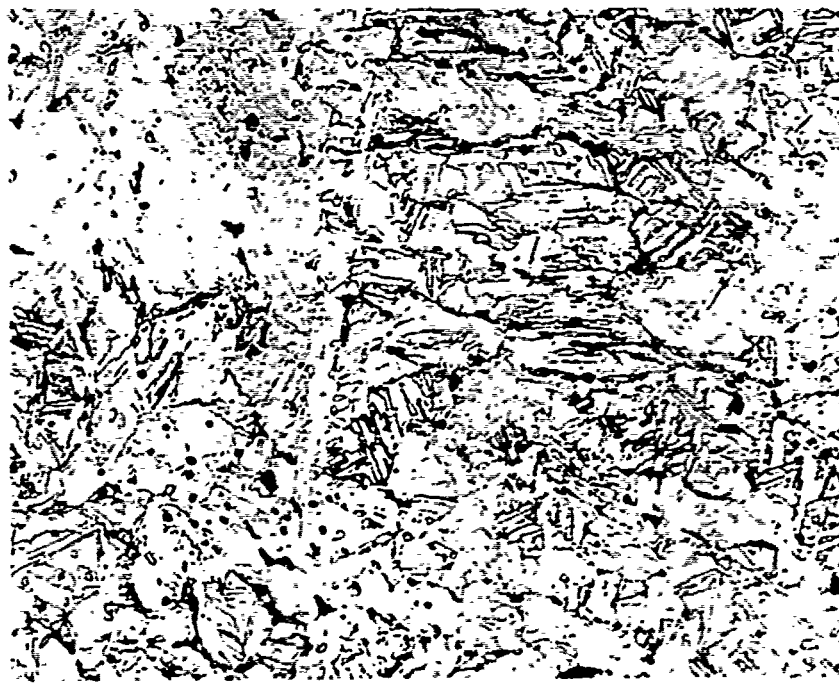


Figure 22. Contains the structure of the 17-4 pH stainless steel base outside of the HAZ. Mag. 200X



Figure 23. Shows the microstructure of the base within the HAZ which was predominantly martensitic with islands of ferrite. Mag. 200X

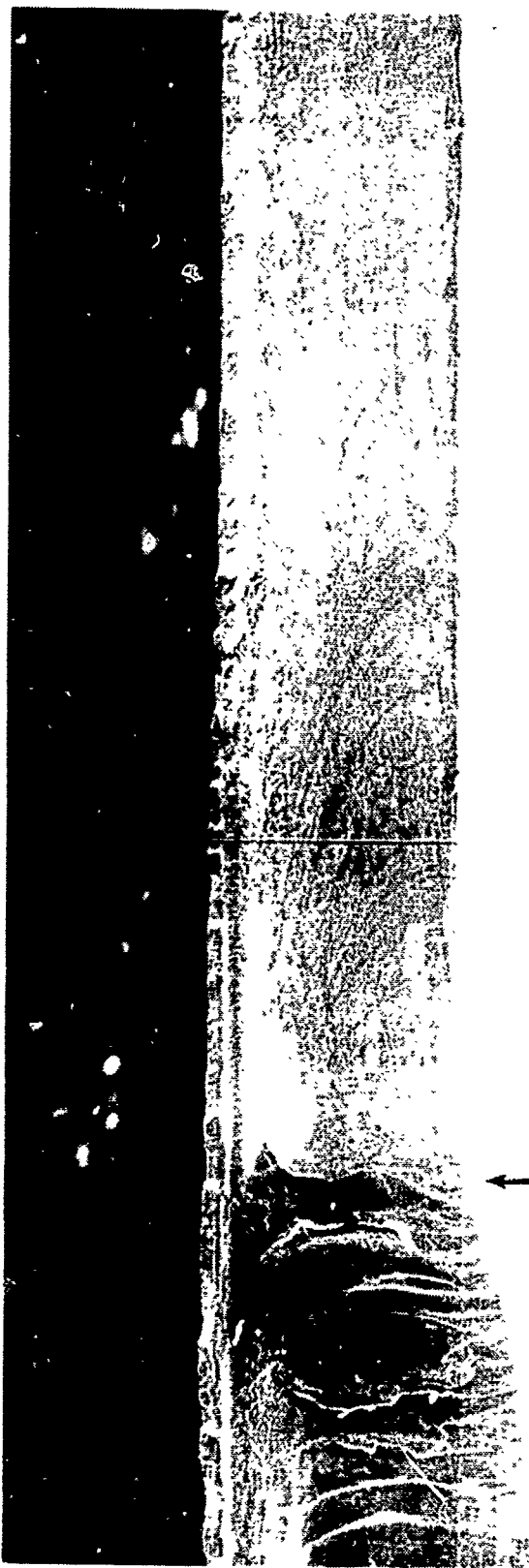


Figure 24. SEM photograph showing the fracture surface within area 1 (identified previously on Figure 14). Mag. 50X



Figure 25. SEM fractograph of area 2 located near weld bead no. 2 showing beach marks. Mag. 50X

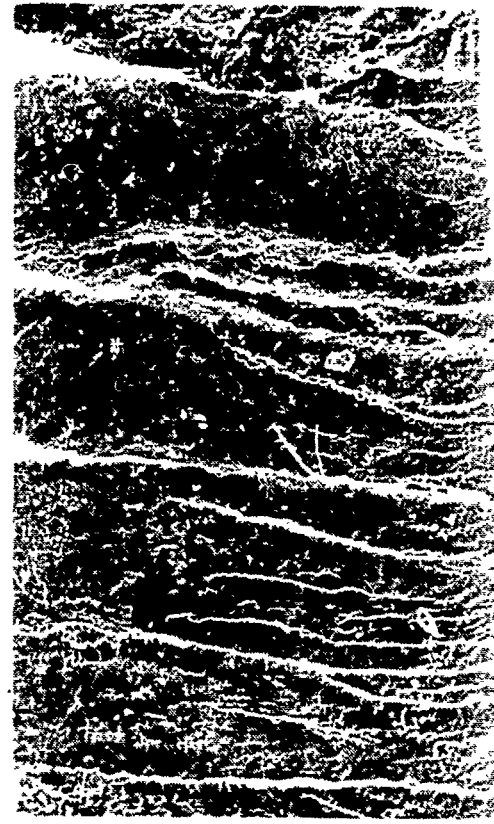


Figure 26. SEM micrograph revealing fracture patterns left behind by the advancing crack front. Mag. 100X

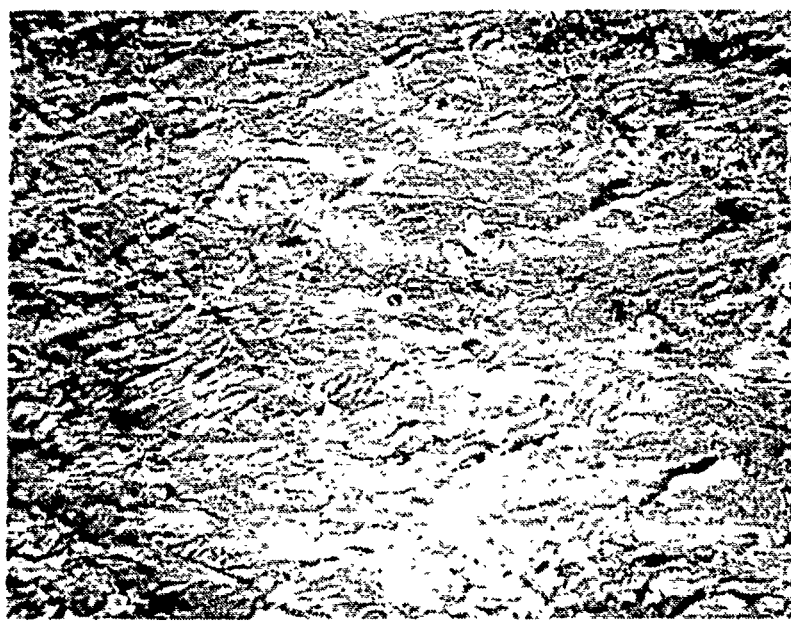


Figure 27. Confirms that the fracture mode was transgranular near the crack origin. Mag. 1KX

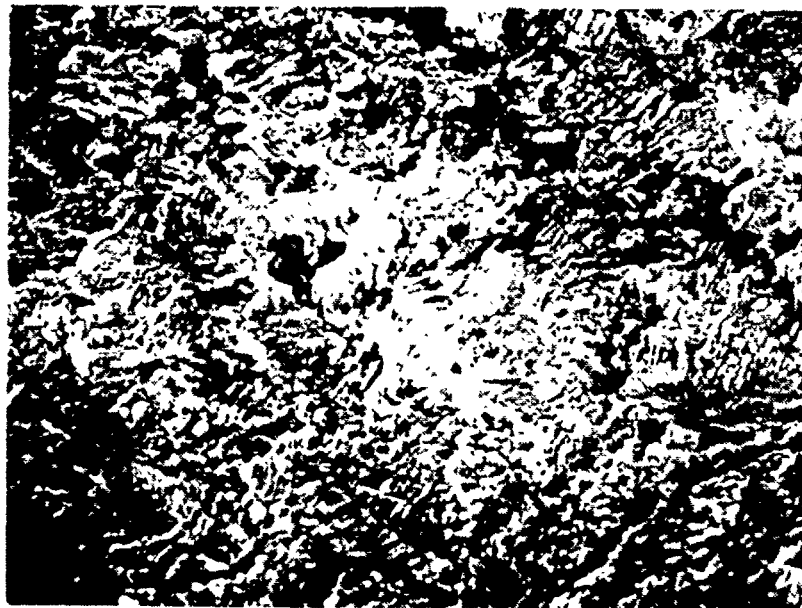


Figure 28. Shows patches of striations on the transgranular fracture surface. Mag. 1KX

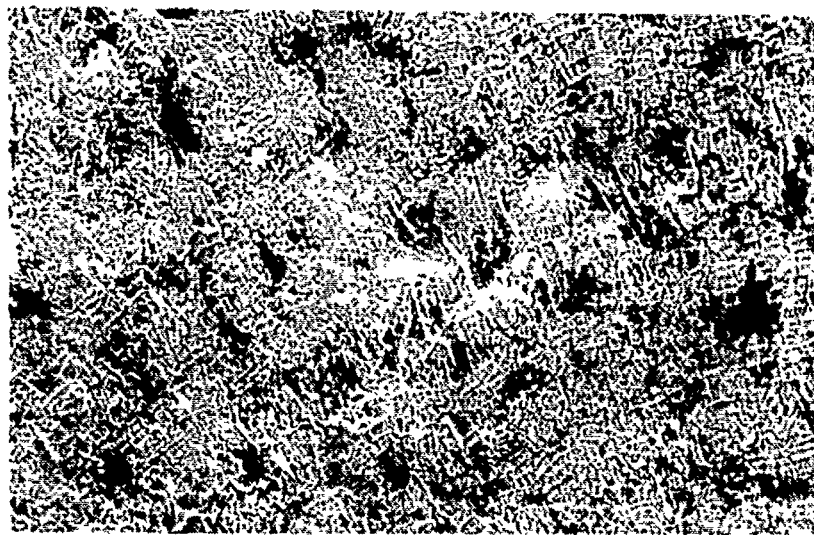


Figure 29. SEM fractograph verifying the existence of fatigue striations.
Mag. 500X

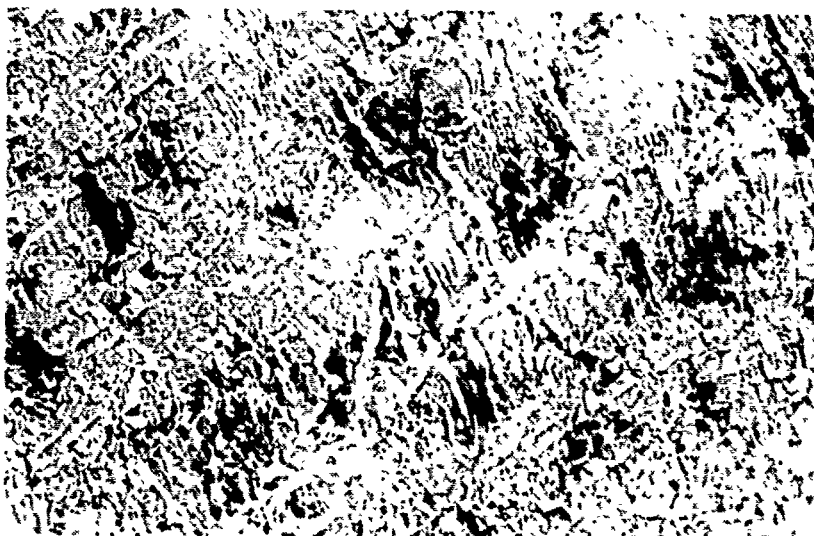


Figure 30. Higher magnification of striations contained in Figure 24.
Mag. 1KX



Figure 31. Still higher magnification of the same striations which occurred during a single cycle of stress. Mag. 5KX

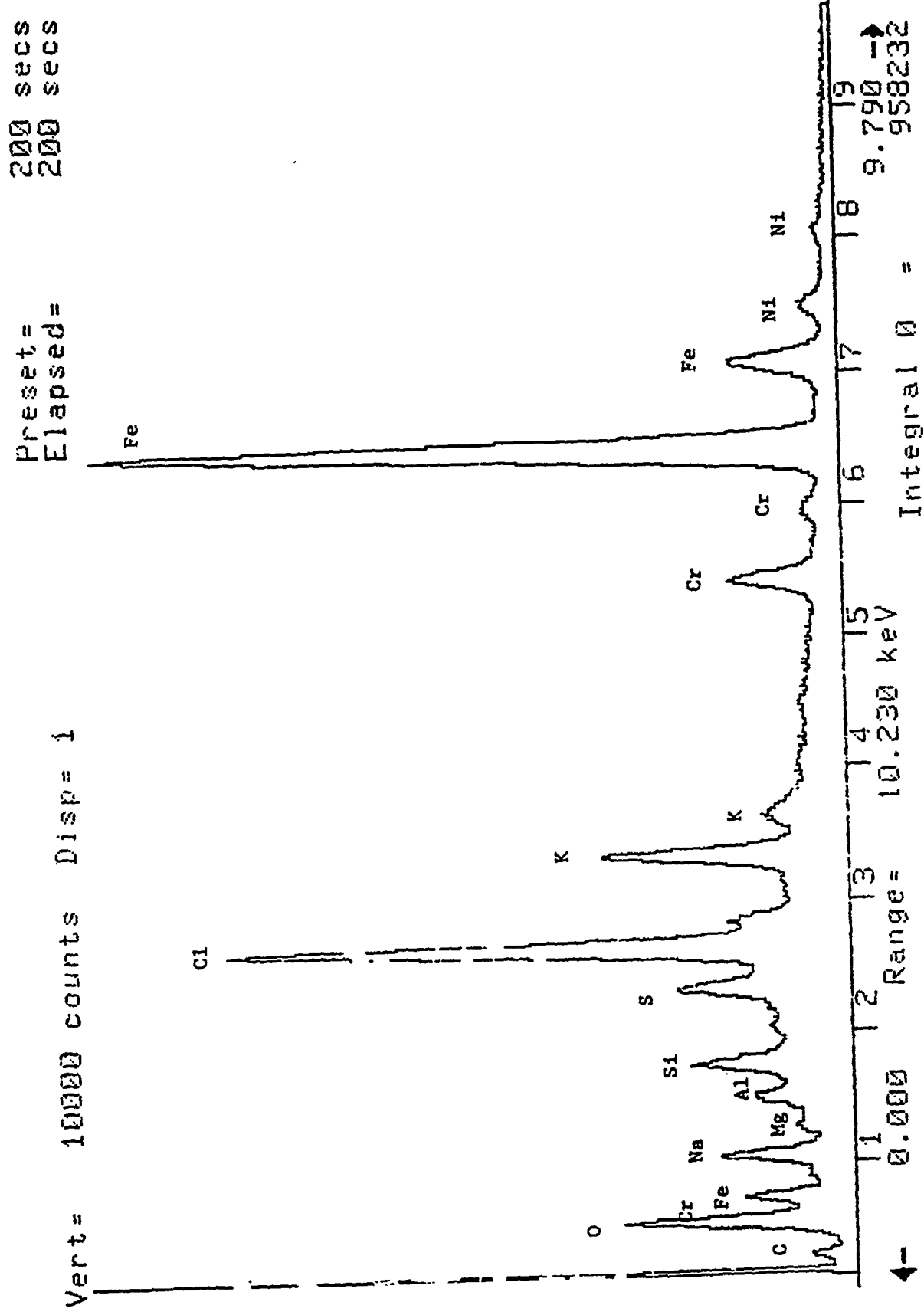


Figure 32. EDS spectra of dark corrosion spots within the fatigue region.

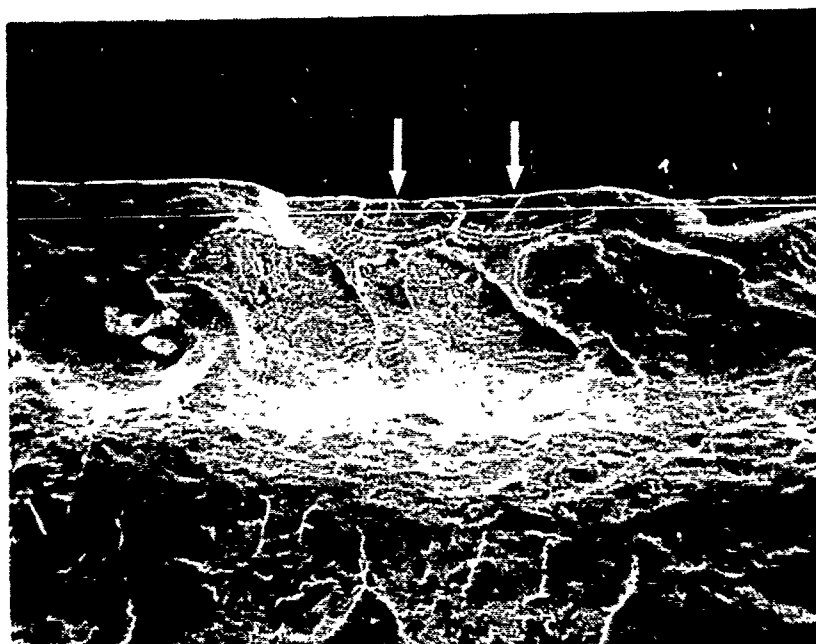


Figure 33. SEM fractograph of area 3 where multiple crack sites were found. Mag. 500X

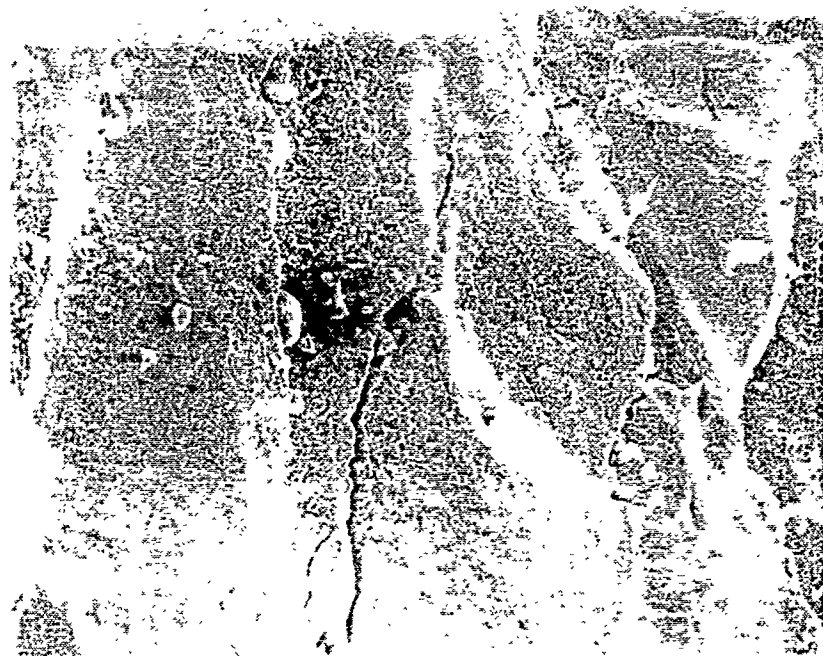


Figure 34. SEM micrograph showing secondary crack
...thin the weld beads. Mag. 400X

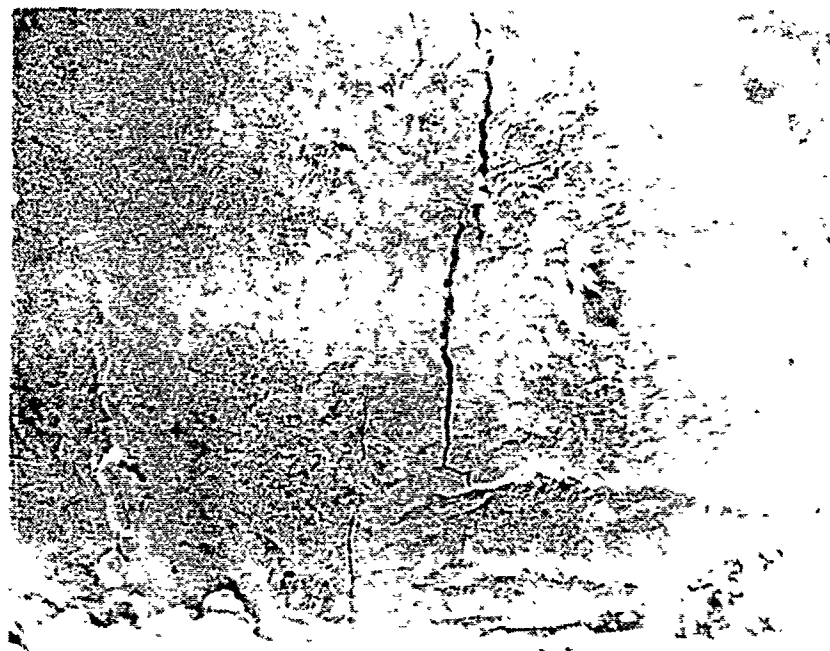


Figure 35. SEM micrograph showing secondary crack
within the weld bead. Mag. 500X



Figure 36. SEM fractograph of the faint beach marks observed in area 4 of weld bead no. 3. Mag. 50X

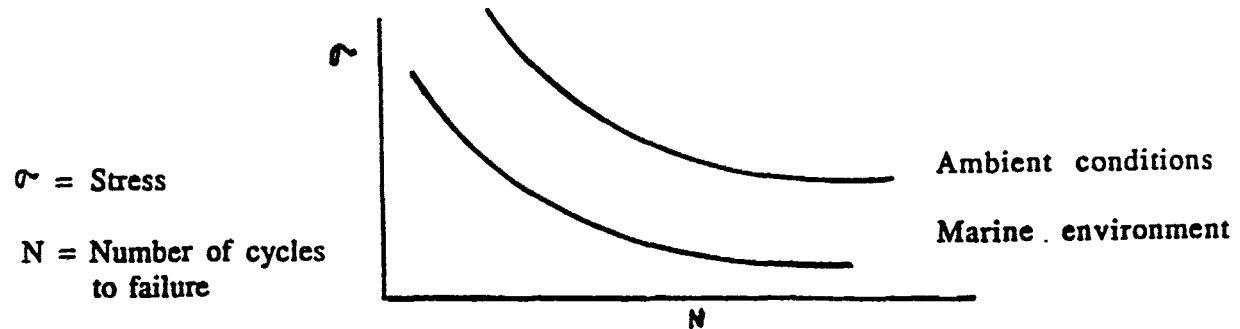


Figure 37. Graph showing the detrimental effects of corrosion on the fatigue life of a material.

DISTRIBUTION LIST

No. of
Copies

To

1 Office of the Under Secretary of Defense for Research and Engineering, The Pentagon, Washington, DC 20301

Metals and Ceramics Information Center, Battelle Columbus Laboratories, 505 King Avenue, Columbus, OH 43201

1 ATTN: Sharad Pednekar

Commander, Defense Technical Information Center, Cameron Station, Bldg. 5, 5010 Duke Street, Alexandria VA 22304-6145

2 ATTN: DTIC-FDAC

Commander, U.S. Army Materiel Command, 5001 Eisenhower Avenue, Alexandria, VA 22333

1 ATTN: AMCQA-P, S. J. Lorber

Commander, Pacific Missile Test Center, Point Mugu, CA 93042

1 ATTN: Sam Keller, Code 2043

1 Bill McAuley (Code 2043)

1 John Durda, Code 2041

1 Carl Louck, Code 2041

1 John Piercy, Code 2041

Commander, U.S. Army Laboratory Command, 2800 Powder Mill Road, Adelphi, MD 20783-1145

1 ATTN: AMSLC-IM-TL

1 AMSLC-CT

Commander, Rock Island Arsenal, Headquarters AMCCOM, Rock Island, IL 61299-6000

1 ATTN: AMSMC-PCA-WM, Joe Wells

1 AMSMC-QAM-I, Gary Smith

1 AMSMC-ASR-M, Brian Kunkel

1 John Housseman

Commander, U.S. Army Test and Evaluation Command, Aberdeen Proving Ground, MD 21005

1 ATTN: Library

Commander, U.S. Army Engineer School, Fort Belvoir, VA 22060

1 ATTN: Library

Naval Air Systems Command, Department of the Navy, Washington, DC 20360

1 ATTN: AIR-03PAF

Naval Research Laboratory, Washington, DC 20375

1 ATTN: Code 5830

Naval Air Development Center, Warminster, PA 18974

1 ATTN: Library

No. of Copies	To
---------------	----

Commander, U.S. Army Aviation Systems Command (AVSCOM) St. Louis,
MO 63120-1798

1 ATTN: AMSAV-ECC, Emanuel Buelter
1 AMSAV-ECC, Robert Lawyer
1 AMSAV-EFM, Frank Barhorst
1 AMSAV-EFM, Kirit Bhansali
1 AMSAV-E, Carl Smith
1 AMCPM-AAH, Dave Roby
1 AMCPM-AAH, Bob Kennedy

Commander, Corpus Christi Army Depot, Corpus Christi, TX 78419-6195

1 ATTN: AMSAV-MRPD, Nicholas Hurta, Mail Stop 55
1 AMSAV-MRPD, Lou Neri, Mail Stop 55
1 SDSCC-QLM, David Garcia, Mail Stop 27
1 SDSCC-QLM, Charlie Wilson, Mail Stop 27

Commander, Armament Research, Development and Engineering Center,
Picatinny Arsenal, NJ 07806-5000

1 ATTN: SMCAR-CCS-C, Anthony Sebasto, Bldg. #1

Program Manager, Government-Industry Data Exchange, GIDEP Operations Center,
Corona, CA 91720-2000

1 ATTN: J. C. Richards, Program Director

Director, U.S. Army Materials Technology Laboratory, Watertown, MA 02172-0001

2 ATTN: SLCMT-TML
3 Authors

U.S. Army Materials Technology Laboratory
Watertown, Massachusetts 02172-0001
Victor K. Champagne, Jr., Gary Wechsler,
and Daniel A. Nowak - FAILURE ANALYSIS OF THE
LAU-7/A LAUNCHER RETENTION BAND ASSEMBLY

Technical Report MTL TR 90-53, November 1990, 31 pp.
illus-tables

AD UNCLASSIFIED
UNLIMITED DISTRIBUTION
Key Words

U.S. Army Materials Technology Laboratory
Watertown, Massachusetts 02172-0001
Victor K. Champagne, Jr., Gary Wechsler,
and Daniel A. Nowak - FAILURE ANALYSIS OF THE
LAU-7/A LAUNCHER RETENTION BAND ASSEMBLY

Technical Report MTL TR 90-53, November 1990, 31 pp.
illus-tables

AD UNCLASSIFIED
UNLIMITED DISTRIBUTION
Key Words

The U.S. Army Materials Technology Laboratory (MTL) conducted a comprehensive metallurgical examination of the launcher retention band assembly to determine the probable cause of failure. The assembly secures the all and of a nitrogen receiver which is part of the LAU-7/A Guided Missile Launcher located on the FA-1B Navy Jet. The retention band failed near the weld joint during service. Visual inspection of the assembly revealed areas conducive to crevice corrosion. Deep depressions produced by the spot welding procedure were found on the surface of the base. Wear and galling marks that were caused by fasteners that had bottomed out on the surface of the band were observed. Light optical microscopy of the fracture surfaces verified the existence of beach marks. It was determined by metallographic examination that the microstructure of the type 17-4 precipitation hardener (PH) stainless steel retention base was predominantly tempered martensite with islands of ferrite while the type 301 stainless steel band showed signs of prior cold working. There was no evidence of excessive carbide formation near the weld. Chemical analysis confirmed that the retention base and band were fabricated from the specified stainless steels, AMS 5355 and ASTM A566 respectively. Hardness testing of the base showed that the minimum hardness requirement of HRC 40 was satisfied. Fractographic analysis revealed beach marks and fatigue striations. The fracture progressed in a transgranular fashion and multiple crack origins were located on the exterior surface of the band. The failure was attributed to fatigue which resulted from the combined effects of poor spot welding, excessive tensile stresses caused by fasteners which bottomed out onto the surface of the band and finally the severe service conditions. The launchers have been relocated on the aircraft and are now installed on the wing tips. In this area the components are subjected to increased vibration and a more corrosive environment during service.

The U.S. Army Materials Technology Laboratory (MTL) conducted a comprehensive metallurgical examination of the launcher retention band assembly to determine the probable cause of failure. The assembly secures the all and of a nitrogen receiver which is part of the LAU-7/A Guided Missile Launcher located on the FA-1B Navy Jet. The retention band failed near the weld joint during service. Visual inspection of the assembly revealed areas conducive to crevice corrosion. Deep depressions produced by the spot welding procedure were found on the surface of the base. Wear and galling marks that were caused by fasteners that had bottomed out on the surface of the band were observed. Light optical microscopy of the fracture surfaces verified the existence of beach marks. It was determined by metallographic examination that the microstructure of the type 17-4 precipitation hardener (PH) stainless steel retention base was predominantly tempered martensite with islands of ferrite while the type 301 stainless steel band showed signs of prior cold working. There was no evidence of excessive carbide formation near the weld. Chemical analysis confirmed that the retention base and band were fabricated from the specified stainless steels, AMS 5355 and ASTM A566 respectively. Hardness testing of the base showed that the minimum hardness requirement of HRC 40 was satisfied. Fractographic analysis revealed beach marks and fatigue striations. The fracture progressed in a transgranular fashion and multiple crack origins were located on the exterior surface of the band. The failure was attributed to fatigue which resulted from the combined effects of poor spot welding, excessive tensile stresses caused by fasteners which bottomed out onto the surface of the band and finally the severe service conditions. The launchers have been relocated on the aircraft and are now installed on the wing tips. In this area the components are subjected to increased vibration and a more corrosive environment during service.

AD UNCLASSIFIED
UNLIMITED DISTRIBUTION
Key Words

U.S. Army Materials Technology Laboratory
Watertown, Massachusetts 02172-0001
Victor K. Champagne, Jr., Gary Wechsler,
and Daniel A. Nowak - FAILURE ANALYSIS OF THE
LAU-7/A LAUNCHER RETENTION BAND ASSEMBLY

Technical Report MTL TR 90-53, November 1990, 31 pp.
illus-tables

AD UNCLASSIFIED
UNLIMITED DISTRIBUTION
Key Words

The U.S. Army Materials Technology Laboratory (MTL) conducted a comprehensive metallurgical examination of the launcher retention band assembly to determine the probable cause of failure. The assembly secures the all and of a nitrogen receiver which is part of the LAU-7/A Guided Missile Launcher located on the FA-1B Navy Jet. The retention band failed near the weld joint during service. Visual inspection of the assembly revealed areas conducive to crevice corrosion. Deep depressions produced by the spot welding procedure were found on the surface of the base. Wear and galling marks that were caused by fasteners that had bottomed out on the surface of the band were observed. Light optical microscopy of the fracture surfaces verified the existence of beach marks. It was determined by metallographic examination that the microstructure of the type 17-4 precipitation hardener (PH) stainless steel retention base was predominantly tempered martensite with islands of ferrite while the type 301 stainless steel band showed signs of prior cold working. There was no evidence of excessive carbide formation near the weld. Chemical analysis confirmed that the retention base and band were fabricated from the specified stainless steels, AMS 5355 and ASTM A566 respectively. Hardness testing of the base showed that the minimum hardness requirement of HRC 40 was satisfied. Fractographic analysis revealed beach marks and fatigue striations. The fracture progressed in a transgranular fashion and multiple crack origins were located on the exterior surface of the band. The failure was attributed to fatigue which resulted from the combined effects of poor spot welding, excessive tensile stresses caused by fasteners which bottomed out onto the surface of the band and finally the severe service conditions. The launchers have been relocated on the aircraft and are now installed on the wing tips. In this area the components are subjected to increased vibration and a more corrosive environment during service.

The U.S. Army Materials Technology Laboratory (MTL) conducted a comprehensive metallurgical examination of the launcher retention band assembly to determine the probable cause of failure. The assembly secures the all and of a nitrogen receiver which is part of the LAU-7/A Guided Missile Launcher located on the FA-1B Navy Jet. The retention band failed near the weld joint during service. Visual inspection of the assembly revealed areas conducive to crevice corrosion. Deep depressions produced by the spot welding procedure were found on the surface of the base. Wear and galling marks that were caused by fasteners that had bottomed out on the surface of the band were observed. Light optical microscopy of the fracture surfaces verified the existence of beach marks. It was determined by metallographic examination that the microstructure of the type 17-4 precipitation hardener (PH) stainless steel retention base was predominantly tempered martensite with islands of ferrite while the type 301 stainless steel band showed signs of prior cold working. There was no evidence of excessive carbide formation near the weld. Chemical analysis confirmed that the retention base and band were fabricated from the specified stainless steels, AMS 5355 and ASTM A566 respectively. Hardness testing of the base showed that the minimum hardness requirement of HRC 40 was satisfied. Fractographic analysis revealed beach marks and fatigue striations. The fracture progressed in a transgranular fashion and multiple crack origins were located on the exterior surface of the band. The failure was attributed to fatigue which resulted from the combined effects of poor spot welding, excessive tensile stresses caused by fasteners which bottomed out onto the surface of the band and finally the severe service conditions. The launchers have been relocated on the aircraft and are now installed on the wing tips. In this area the components are subjected to increased vibration and a more corrosive environment during service.